Int. J. Rock Mech. Min. Sci. & Geomech. Abstr. Vol. 11, pp. 139–150. Pergamon Press 1974. Printed in Great Britain

Direct Observation of Microcavities in Crystalline Rocks

EVE S. SPRUNT
W. F. BRACE*

Removal of about 30 μm of material from a polished surface by ion thinning reveals microcavities in granite, diabase or gabbro as they exist in the interior of the material. A string of long, thin low aspect ratio cavities often follows grain boundaries in granites; aspect ratio of cavities ranges down to 10^{-3}. In all rock types studied, individual low aspect ratio cavities rarely exceed about a tenth the grain size contrary to theoretical predictions. The strings of cavities could be partially healed early fractures. Nearly equant cavities up to several μm in size are very abundant in sodic plagioclase, less common in quartz and potash feldspar, and irregularly distributed along grain boundaries. They could be the sites of fluids remaining after crystallization, traces of original porosity, or the remains of healed cracks. Mechanical or thermal stress introduces sharp-ended brittle cracks and other more subtle damage near the ends of longer cavities. Accurate mapping of crack-like cavities in most unstressed rocks will require ion-thinned samples and the SEM.

INTRODUCTION

Nearly all rocks, even dense, crystalline varieties such as granite, dunite or quartzite contain tiny cavities which may amount to a percent or so by volume. As first recognized by Adams and Williamson [1], cavities in the form of cracks may profoundly influence elastic properties of rocks like granite. The role played by cracks and more nearly equant cavities called pores was later related not only to elastic, but to electrical, transport, thermal and strength characteristics as well (summarized in [2]). In spite of the importance thus ascribed to what we will term *microcavities*, only in rare cases have their actual form and distribution been observed. Direct observation is difficult, in part, because of small size. Also, to view material in the interior of a rock sample, one has to prepare a section; to date this has been a standard thin or polished section. During preparation of a section, new cracks and other surface damage are inevitable. For these reasons, detailed observation of the microcavities in rocks has enjoyed little success, and parameters like crack aspect ratio, density or connectivity have, we feel, never been unambiguously determined.

We described briefly a new technique [3] which appeared to overcome the difficulties noted above; the key feature was preparation of the surface to be viewed by ion thinning. One could then view microcavities with the scanning electron microscope (SEM) and gain both the advantages of a damage-free section and the high magnification needed to accurate characterize cracks and pores. In the present paper, we supply additional details of the technique, we illustrate typical microcavities in stressed and unstressed rocks, and discuss a number of implications, both petrologic and mechanical, of this first close-up view of cracks and pores [4].

PREVIOUS STUDIES

Several attempts have been made to observe and map cracks in rocks using thin or polished sections. In some cases, an effort was made to decorate pre-existing cavities so that they could later be distinguished from those introduced by sectioning.

Paulding [5] observed many transgranular cracks in thin sections of undeformed Westerly granite. For samples stressed in triaxial compression, his thin sections revealed that transgranular cracks became more abundant, starting at a stress close to half the fracture strength.

Koide and Hoshino [6] investigated microfractures in experimentally deformed rocks using thin sections. Their criteria for an open crack was one that appeared dark under crossed nicols and clear under uncrossed nicols. From their study they obtained the preferred orientation of microcracks. Peng and Johnson [7] determined length, distribution and preferred orientation of microcracks in granite from thin section. A microcrack was defined as an open fissure as viewed with a petrographic microscope. Willard and McWilliams [8] determined the orientation of defects in thin sections, including grain boundaries, cleavage planes, twin planes, slip planes, inclusion planes, deformation bands and microfractures. Orientation of all cracks was recorded irrespective of origin. Wawersik and Brace [9] used polished sections to study crack density, crack orientation, crack location relative to grain boundaries, and orientation of the longer partial fractures in stressed rocks. They noted the

* Department of Earth and Planetary Sciences, Massachusetts Institute of Technology, Cambridge, Massachusetts 02139, U.S.A.

difficulty in distinguishing cracked from uncracked grain boundaries.

Baldridge and Simmons [10] studied cracks in quartzite with two types of decoration. One was based on the yellow coloration of Canada Balsam. The other followed the scheme of Fryer and Roberts [11]; a mixture of furfuryl alcohol and acid was injected into cracks. The mixture then polymerized and the impregnated sample was heated to 750°C to convert the polymer to carbon. Submicron sized particles of carbon supposedly identified the cracks after sectioning. They reported crack densities, crack orientations, average lengths, and crack intersections. Hadley [12] attempted audioradiographic crack mapping using tritiated furfuryl alcohol.

Timur *et al.* [13] used the SEM to observe samples prepared with conventional polishing techniques. Although primarily concerned with the structure of pores in sedimentary rocks, they showed photomicrographs of cracks and pores in a granite.

If we assume that the principal goal in the above studies was a detailed description of cracks or pores as they occur within rock, then most of them probably fall far short of their objective. Based on details now apparent using ion thinning and SEM [3], we believe that many of the features reported above represent surface damage acquired during sectioning. As it turns out, most of the microcavities are on the same scale as or smaller than the damaged surface layer; even apart from damage, their scale is such that, decorated or not, they are probably below the resolution of most optical equipment. We will return to this point following presentation of our results.

ROCKS STUDIED

The rocks studied are listed in Table 1 in order of increasing total porosity. Total porosity and crack porosity were determined as in [14]; pore porosity is simply the difference. Where no reference is given in Table 1, a new determination was made. Many of the rocks were used in previous studies; in general we list the most recent of these. The diabase is from the same block used by Birch [15] and referred to as diabase I in [16]. The Westerly granite is from the block known as G-1 [15]. We used the porosities determined on similar blocks used in [14] and subsequent studies. We collected the Raymond and Chelmsford granites; the Red Lake and Katahdin rocks were supplied by Harold Noyes and Rudolf Hon, respectively, of M.I.T. The Chelmsford block is from the same quarry as material used in [15] and [17].

The actual samples were, with the exception of the Red Lake and Katahdin rocks, in the form of blocks obtained from cut stone quarries. The Red Lake and Katahdin samples were typical hand specimens collected with a hammer. As both come from regions that were recently glaciated, the material is presumably free from weathering.

METHOD

Cores about 1 cm dia. were taken from large blocks. After the ends were ground perpendicular to their axes, the cores varied from 1 to 1·3 cm in length. A groove cut with a diamond saw along the axis of each core served as an origin of coordinates for the end surface during later viewing. Following the above machine grinding, we hand ground the surface to be viewed in the following sequence. About 300–400 μm of rock was removed with increasingly fine silicon carbide abrasives (240, 400 and 600 grit) on a metal wheel, followed by polishing with aluminum oxide abrasives (5, 1 and 0·3 μm) on cloth laps. The next step was the crucial one. A layer about 30–40 μm thick was removed by ion bombardment, also termed ion thinning, in a Commonwealth Scientific ion milling instrument. An ionized argon beam of about 6

TABLE 1. ROCKS STUDIED

Rock	Porosity (%) Crack	Pore	Total	Grain size (μm)	Maximum LARC (μm)	Modal analysis*	Reference
Diabase I Frederick, Md.	0	0·1	0·1	180	30	48 an_{67}, 49 pyr, 1 mica	Brace and Orange [16]
Gabbro San Marcos, Cal.	0	0·2	0·2	2000	180	70 an_{42}, 12 mica, 8 pyr, 7 am, 3 ox	Brace and Orange [16]
Raymond granite Madera, Cal.	0·22	0·4	0·6	2000	180	47 an_{16-20}, 35 qu, 10 mi, 7 mica	
Katahdin granite I Baxter State Park, Maine	0·20	0·7	0·9	2000	260	28 an_{18-24}, 35 qu, 27 mi, 9 mica	
Granite, Westerly Rhode Island	0·20	0·7	0·9	750	100	27·5 qu, 35·4 mi, 31·4 an_{17}, 4·9 mica	Birch [15]
Granite, Chelmsford Massachusetts	0·16	0·9	1·0	1500	150	31 qu, 31 mi, 31 an_{20-24}, 7 mica	
Granodiorite of Red Lake Shaver Lake, Cal.	0·29	0·8	1·1	2000	360	49 an_{30}, 27 mi, 17 qu, 5 mica, 2 misc	
Katahdin granite II Baxter State Park, Maine	0·46	0·8	1·2	3000	600	29 an_{18-24}, 29 qu, 33 mi, 9 bi	

* an = Plagioclase; pyr = pyroxene; ol = olivine; am = amphibole; ox = oxide; qu = quartz; bi = biotite; mi = microcline

kV bombarded the sample at an angle of 17°. Ion thinning is the vital difference between our specimens and the ordinary polished section.

Ion thinning does not produce a perfectly smooth surface because thinning rate depends on mineralogy. Olivine and orthopyroxene thin at about 1 μm/hr, plagioclase at 2 μm/hr, and quartz at 3 to 8 μm/hr. Mica thins even faster than quartz. Thinning time was kept close to the minimum period necessary to remove the damaged layer (6 hr for most rocks) so as to avoid very large topographic steps between different minerals. Thinning also tends to produce dimples, which range in size from about 5 to 50 μm. The dimples appear to bear no relation to grain boundaries or grain defects. Grain boundaries, cracks and pores are not etched out.

Since specimens viewed with a scanning electron microscope (SEM) must have conducting surfaces, approximately 400 Å of a 40 per cent gold 60 per cent palladium alloy was vacuum evaporated onto the surface. Details of our method of relocating precise fields and of our sample holders are given in Sprunt [21]. References on the general use of the SEM include [18–20].

To get a three-dimensional picture of the porosity, some samples were serially sectioned after photographs had been taken of selected fields under the SEM. First the metal coating was removed by hand with 1 and 0·3 μm aluminum oxide abrasives. Then the surface was ion thinned for 6 hr. If polishing did not precede thinning, any small irregularities in the coating seemed to cause very uneven thinning of the rock.

The effects of thermal stress were studied in a sample which, after being prepared as described above and photographed, was placed for 3·5 hr in a furnace at 400°C, which was calculated to be more than sufficient to induce many cracks in the rock. Heating and cooling rates were about 50°/hr. Recoating was unnecessary and the sample could be viewed immediately after removal from the furnace.

The mechanically stressed samples (Table 2) came from dogbone-shaped specimens loaded in triaxial compression [5]. The rocks were recovered intact after being loaded to over 95 per cent of their fracture strength. The specimens were cast in a mold, sawed in half lengthwise, and cores were drilled from their centers. The core surfaces were polished, thinned, and coated, as described above.

TABLE 2. STRESSED ROCKS STUDIED

Rock	Confining pressure (kb)	Strength (kb)	Reference
Westerly granite no. 18	1·5	10·52	Paulding [5]
Westerly granite no. 28	0·5	6·30	Paulding [5]
Maryland diabase	1·6	13·21	Wawersik and Brace [9]

OBSERVATIONS

General

Low magnification fields from Chelmsford (Fig. 1) and Westerly granites (Figs. 2 and 3) somewhat resemble

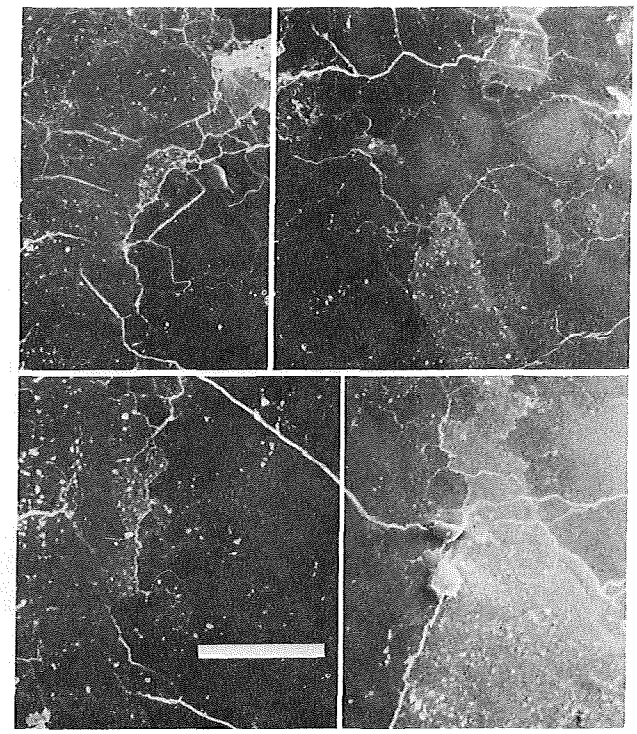

Fig. 1. Low magnification field in thermally stressed Chelmsford granite. The darker areas are generally quartz grains, the light grey, plagioclase. The wavy white lines are rows of low aspect ratio cavities, the white spots, more nearly equant, high aspect ratio cavities. A portion of this field left of center is magnified in Fig. 11. The white bar has a length of 300 μm.

ground surfaces viewed in reflected light. Quartz, microcline and plagioclase are slightly different in color, and grain boundaries at this scale are well defined. Beyond this the resemblance ends. As seen in Fig. 1, the grain boundaries are often marked by wavy white lines and the grain interiors by white spots. At higher magnification (Figs. 2 and 4) these white lines are seen to be a string of narrow cavities and the spots to be pits or holes. The exact location of the boundary is often unclear (Fig. 4). Unlike a polished surface, the surface produced by ion thinning has considerable topography when viewed at high magnification. Grain boundaries are often close to a sloping step in the surface (for example between quartz and plagioclase in Figs. 3 and 4), and the surface in general is often covered with dimples (Figs. 2–4) as noted above.

The light color associated with both cavity edges and sharp topographic steps may be explained by secondary electrons which, in these areas, have an unusually large surface through which they can escape. The center of a cavity is dark because of the failure of electrons from a depressed area to reach the collector [18, 20]. To judge from photomicrographs published elsewhere [13], the contrast in brightness near a cavity or step depends somewhat on the particular SEM used and on the operator's choice of contrast. In our case, the contrast greatly facilitated the location of microcavities.

Exact location of microcavities relative to grain boundaries was one aim of our study. On a gross scale (Fig.

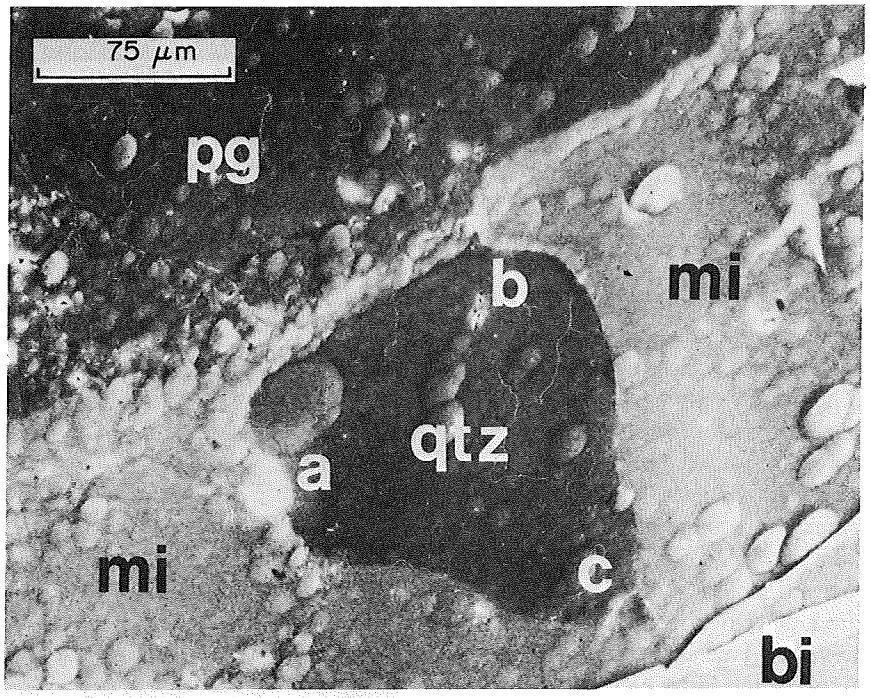

Fig. 2. Photomicrograph of a multigrain field in Westerly granite. The center quartz (qtz) grain is surrounded by microcline (mi), biotite (bi) and plagioclase (pg) grains. The bright areas at 'a', 'b', and 'c' are cracks which occupy about 20 per cent of the quartz grain boundary. The irregular mounds are from ion thinning.

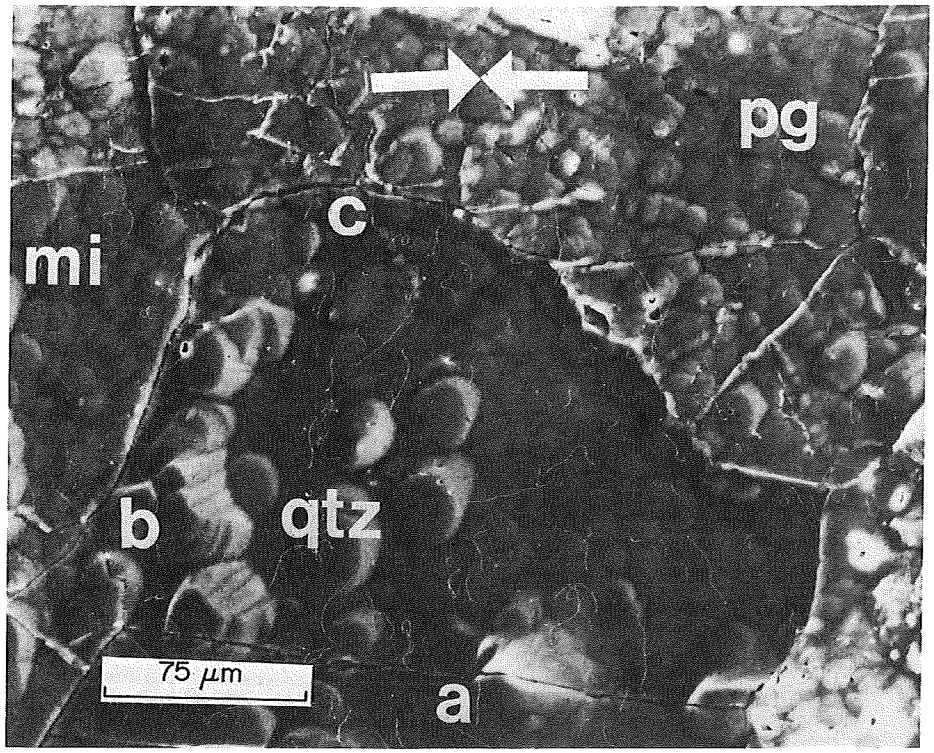

Fig. 3. Photomicrograph of Westerly granite (no. 18) which was stressed in triaxial compression to over 95 per cent of its fracture strength. The white arrows show the direction of maximum compression.

1, for example) it was often clear that a row of slots marked the boundary of two grains. However, in detail (Fig. 4, for example), we could seldom locate a boundary to within 5 or 10 μm. Also, under the SEM two grains of, say quartz, appear identical so that it was unclear whether certain cavities separated two grains or were intragranular. Some effort was made to locate grain boundaries with the electron microprobe [21], but resolution better than the above limits was not attained.

Cavities down to about 0·02 μm (200 Å) wide could be resolved with our SEM. Several factors limited resolution, among them the 400 Å layer of metallic coating needed for viewing the surface of a rock in the SEM. The range of magnification used was 100–30,000 times.

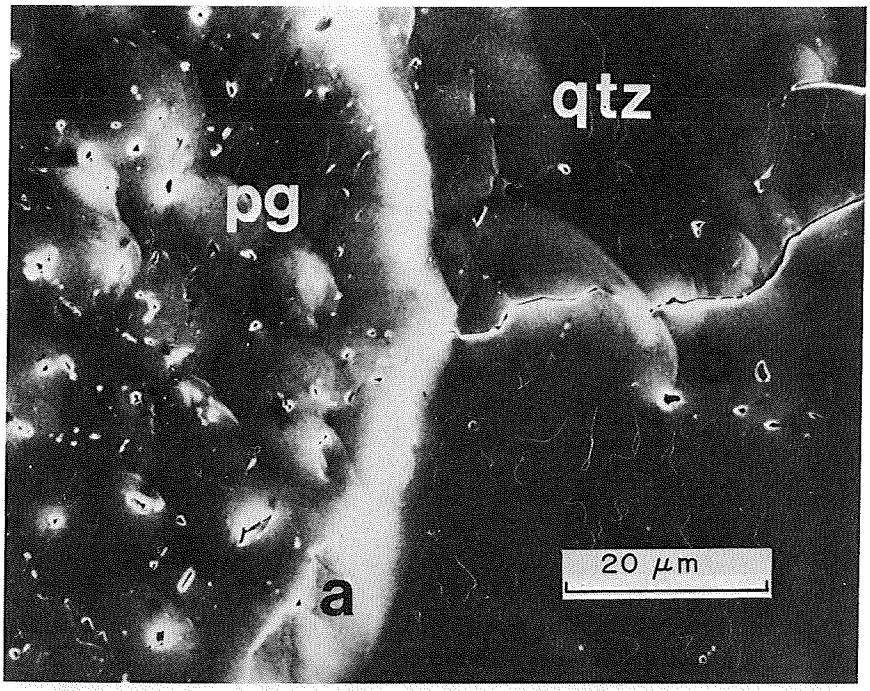

Fig. 4. High magnification of a quartz–feldspar grain boundary in unstressed Chelmsford granite. The porous aspect of sodic plagioclase (pg) shown here is typical as is the low density of high aspect ratio cavities in quartz. An irregular string of low aspect ratio cavities follows a topographic step marking the grain boundary at *a* and then passes into the quartz above *b*. The bright band bisecting the picture marks the topographic step.

Another aim of our study was the determination of the three-dimensional form of microcavities, presumably by serial sectioning. This was never satisfactorily achieved owing to the fine scale of most microcavities in rocks. To date we have been unable to section at intervals closer than about 30 μm; a few long cavities have been traced downward [21], but most cavities are lost owing to this wide interval. The observations and discussion in this

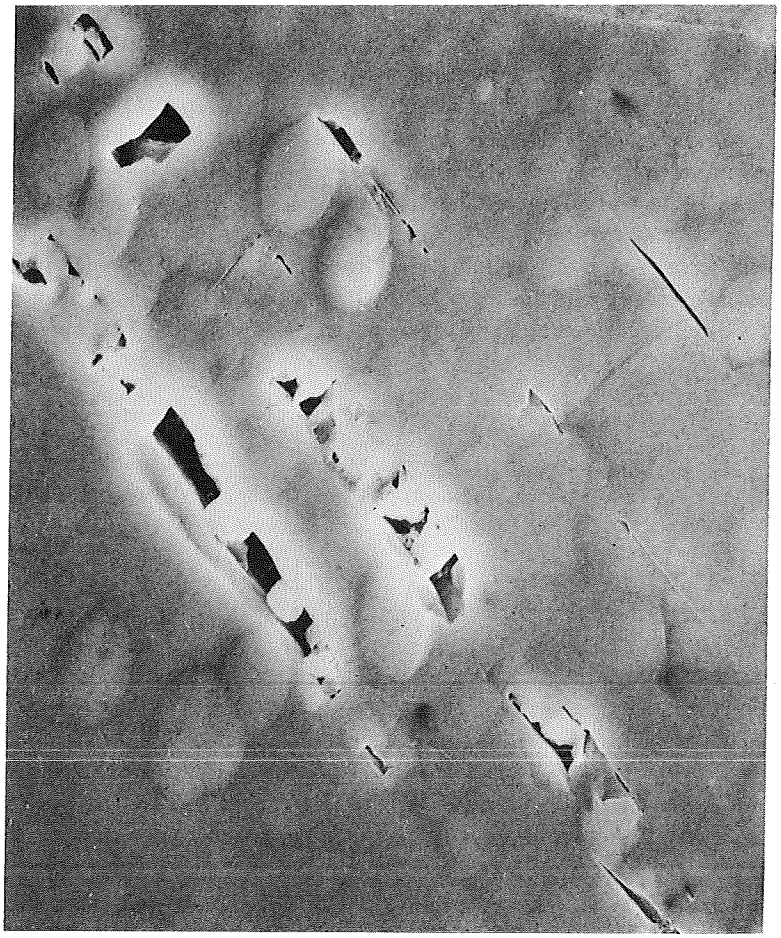

Fig. 5. Cavities at high magnification in plagioclase of Raymond granite. The largest pore seen is 10 μm in length.

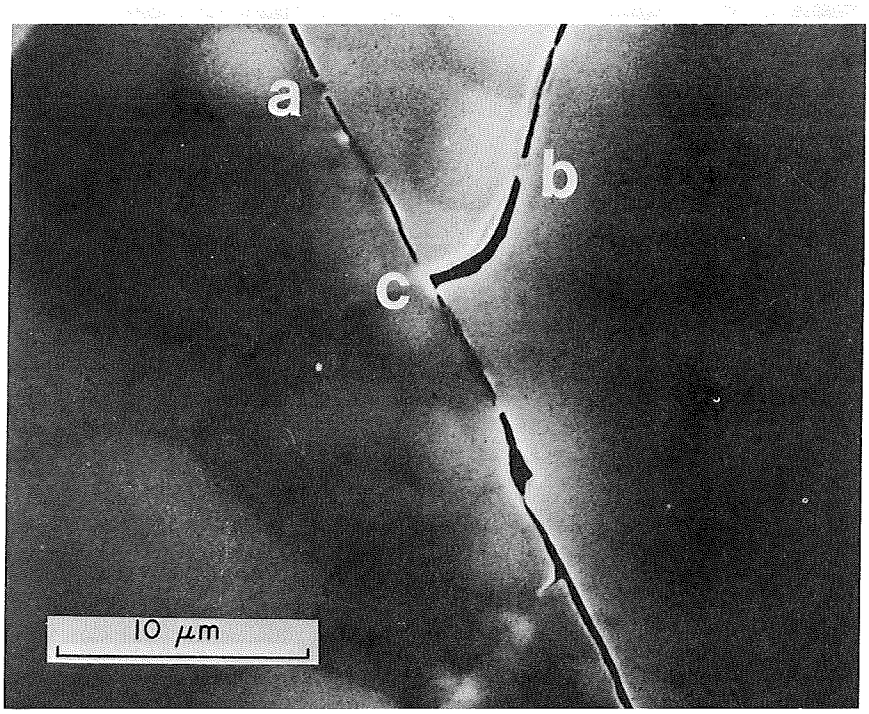

Fig. 6. Typical string of low aspect ratio cavities, associated with quartz grains in Westerly granite. Typical bridges are at a, b and c. Note the blunt, often rounded ends of cavities.

paper, therefore, pertain solely to the two-dimensional aspect of microcavities. Clearly, extension to three dimensions deserves further attention.

Microcavities

At high magnification, many of the bright spots and wavy lines in a field such as Fig. 1 are seen to be open cavities (Figs. 3–6, for example) whose cross-sections have various shapes. Some are long and crack-like, some are slot-like with rounded or blunt ends, some are circular or triangular, and some are, simply, irregular. The length of 80 of these cavity cross-sections selected randomly in unstressed Westerly granite had the distribution shown in Fig. 7. If we define *aspect ratio*, α, of a cross-section as the ratio of minimum to maximum opening, then the frequency distribution of α is shown in Fig. 8. Evidently the majority of cavities are nearly equant in cross-section; cavities with α ranging from 10^{-1} to 10^{-4} are about equally abundant. An α of 10^{-1} will serve as the division between what we will term *high aspect ratio cavities* (HARC) and *low aspect ratio cavities* (LARC) in the sections to follow.

LARCs

Long, narrow, sharp-ended cracks, typical of brittle fracture, are relatively rare in the rocks we examined; they are almost never seen in unstressed samples. One example is shown in Fig. 9 for mechanically stressed dia-

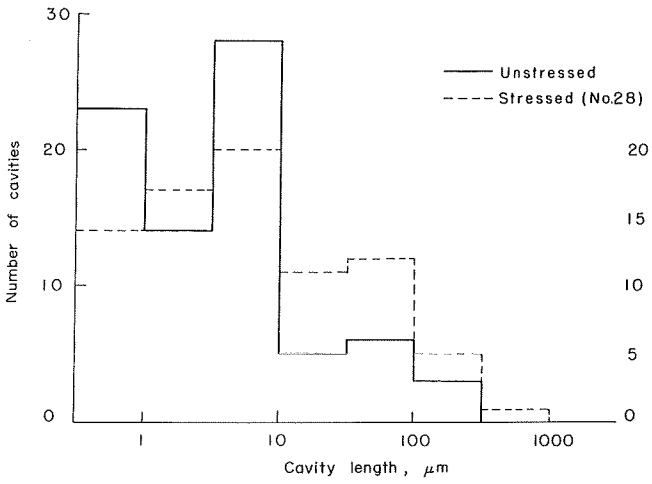

Fig. 7. Frequency distribution of cavity length in stressed and unstressed Westerly granite. The samples contained 80 randomly selected cavities.

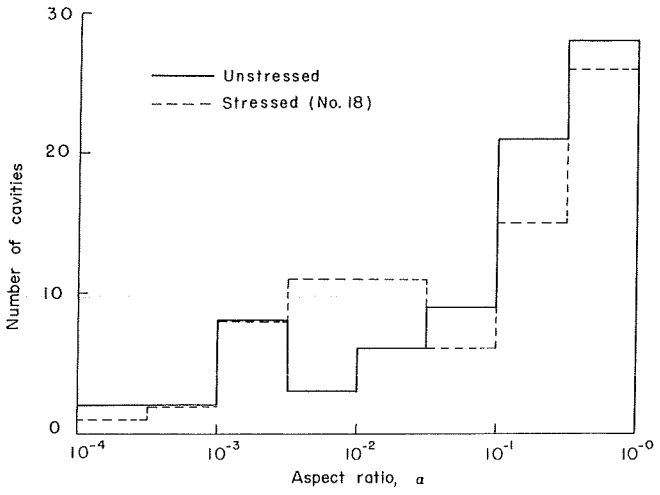

Fig. 8. Frequency distribution of cavity aspect ratio in unstressed and stressed Westerly granite. In each a random sample of 80 cavities was compared.

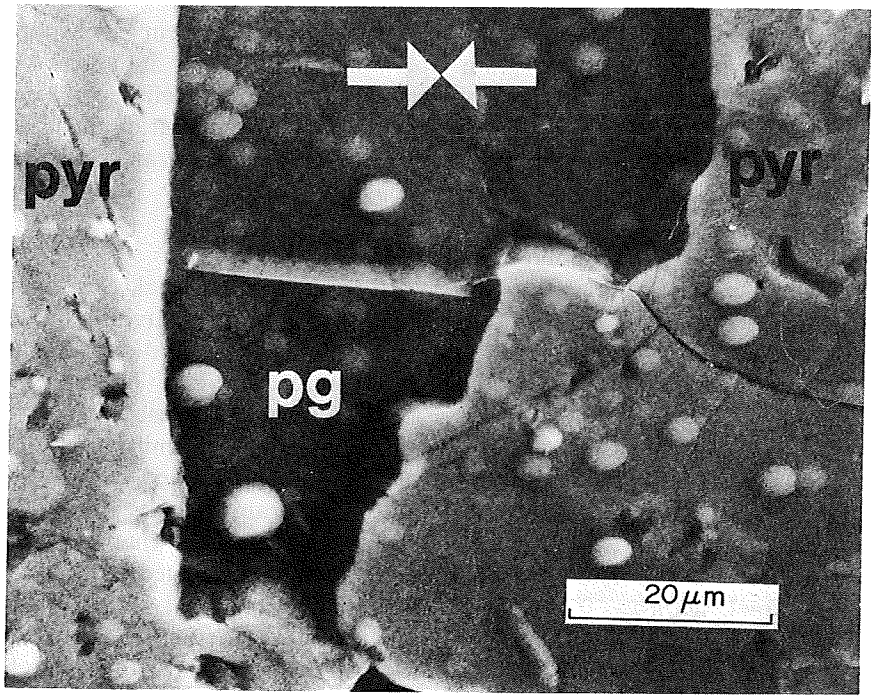

Fig. 9. High magnification photomicrograph of stressed diabase showing prominent brittle crack which crosses the plagioclase–pyroxene grain boundary. The arrows give the direction of the maximum compression. The marked topographic step is apparent at the grain boundary as is the system of very fine cracks emanating from the larger one in pyroxene.

base; a crack-like feature crosses a plagioclase-pyroxene boundary. As discussed below, tiny crack-like features are also observed in thermally stressed rocks.

The long wavy white lines seen at low magnification (Fig. 10a) were first thought to be single LARCs. In detail, however, they very commonly proved to be a string of slots as in Figs. 4 and 6, or even rows of nearly equant HARCs as in Fig. 5. The width of LARCs ranges from about 1 μm down to the limit of resolution; length of individual cavities varies somewhat among rocks but ranges up to something less than 1 mm. Maximum LARC length for our unstressed rocks is listed in Table 1 together with grain size. Narrow cavities, around 0·1 μm wide, were associated with low aspect ratio; α for rocks of low crack porosity such as diabase or gabbro was similar and maximum LARC width was about 0·3 μm.

Grain boundaries are preferred sites for LARCs in both stressed and unstressed material, although rare intragranular LARCs cut grains of mica, feldspar (Fig. 5) or pyroxene, presumably along cleavage directions.

One of the most curious aspects of the LARCs is their mode of termination. In unstressed material the ends of most LARCs are blunt, some are circular, and a few even square (Figs. 2 and 6; Fig. 1[3]). Individual LARCs are often bridged by uncracked material (Fig. 6). At low magnification the bridges may not be apparent, so that the row of LARCs appears to be a single long feature. This, of course, complicates the measurement of length or aspect ratio of a cavity; unless the bridges are apparent, the length aspect ratio will be over-estimated. Curvature and sinuosity of a cavity also complicated measurement of length or aspect ratio; we arbitrarily measured length to the point on the cavity where it abruptly changed direction 45° or more.

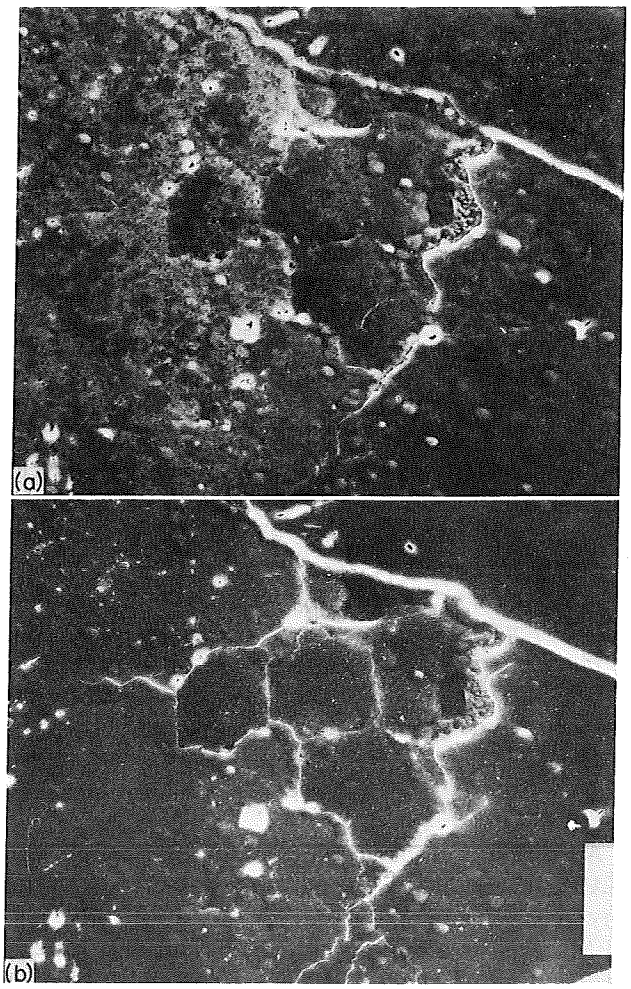

Fig. 10. Photomicrographs of the same field in unstressed (a) and thermally stressed (b) Chelmsford granite from the same area as Fig. 1. Detailed comparison of the two views reveals the extent of damage due to heating this rock to about 400°C. Most new cavities have formed at grain boundaries. Bar length is 60 μm.

The form of the bridges varied somewhat. As shown previously [3], bridges at a feldspar–feldspar grain boundary resembled material splintered from the cavity walls but still attached on both sides. More typically, particularly at quartz boundaries, the end of the cavity had a nearly circular form; the radius was commonly 0·1–0·2 μm (Fig. 6, for example).

The number of LARCs sharing a common point of intersection ranged from 2 to 4 in granite; in gabbro and diabase, cavities were so rare that we observed few intersections. In Red Lake granite, a six-fold intersection seemed to be an upper limit, whereas it was three-fold for Westerly granite.

We tried to estimate the porosity associated with LARCs in a field in Chelmsford granite (the upper two-thirds of the field shown in Fig. 1 before thermal stressing) for comparison with the crack porosity (Table 1). Length and width of all LARCS in this field were measured; the area represented by LARCs was 0·27 per cent of the total area. For cylindrical cracks this would give a crack porosity of 0·27 per cent; the measured value was 0·16. This rather large difference could be explained if the LARCs were more nearly penny-shaped than two-dimensional; it might also be due to the unusual abundance of quartz in the section chosen for analysis. Unfortunately resolution of this difference requires a more detailed three-dimensional picture of microcavities than we can currently obtain.

HARCs

High aspect ratio cavities appear in several configurations, one of which is as scattered cavities, for example below point *b* in the quartz grain in Fig. 2. Some of these HARCs are connected by fine LARCs and others appear isolated in this section. Another configuration, suggesting strong alignment along certain crystallographic direction, is shown (Fig. 5) from Red Lake granite.

Dense concentrations of HARCs in feldspar, especially sodic plagioclase, are common in granite. Three granites, Westerly (an_{17}), Chelmsford (an_{20-25}), and Red Lake (an_{30}) have concentrations of HARCs 7 μm or less in width, with many about 0·4 μm in size. In Katahdin granite I almost all of the plagioclase HARCs are less than 0·7 μm wide, while in Raymond granite many are about 1 μm wide. In Chelmsford granite (Fig. 2) porosity in plagioclase grains due to HARCs amounts to about 2 per cent. The microcline porosity in Chelmsford granite is somewhat less. In Westerly granite the microcline is relatively HARC-free. The plagioclase in San Marcos gabbro (an_{42}) and Maryland diabase (an_{67}) are nearly HARC-free.

An overall estimate of porosity associated with HARCs came close to the measured value of pore porosity for Chelmsford granite. This was done visually for SEM fields from quartz, plagioclase and microcline; it included grain boundary HARCs. The number obtained from a field was assumed to be the volumetric porosity of that phase; rock porosity was obtained using the volume fraction of the phases (Table 1). The rock value obtained in this way was 1·2 per cent; values obtained by immersion of different blocks ranged from 0·9 to 1·0 per cent. Inconsistency in these two comparisons, single crystal and rock, may reflect compensating errors for the rock estimate. Some intragranular HARCs may be isolated, whereas some grain boundary HARCs may be tubular, for example.

Grain boundaries

In unstressed material, the percentage of the grain boundary containing cavities varied significantly from rock to rock. In gabbro and diabase, the grain boundaries were crack-free. Typically, less than half each grain boundary was cracked in Westerly granite. Examination at high magnification of the quartz grain in Westerly granite seen in Fig. 2 showed that about 20 per cent of its grain boundary is cracked; the LARCs all have aspect ratios less than 100 and are located in the bright regions designated *a*, *b* and *c*. In Chelmsford, Raymond and Katahdin I granites more than half of each grain boundary is cracked. Almost all of the grain boundaries in Red Lake and Katahdin II samples are cracked. Even when most of a grain boundary is cracked, the cracking usually consists of many LARCs whose lengths are all much shorter than the apparent grain diameter.

Mechanically stressed rocks

A sharp contrast between stressed (Table 2) and unstressed Westerly granite is apparent in Figs. 2 and 3. In the stressed rock the grain boundary is occupied by LARCs of lengths approaching a grain diameter. At *a* in Fig. 3, a LARC with an aspect ratio of a little more than 200 is located in the grain boundary. At *c* in Fig. 3, cracks run from the grain boundary into the interiors of the grains on both sides. This type of cracking, beginning at the grain boundary, is never seen in the unstressed rock. Multiple crack intersections are common as at *b* and *c* in Fig. 3.

Histograms of cavity length (Fig. 7) and aspect ratio (Fig. 8) reveal that cavities 10–100 μm long have appar-

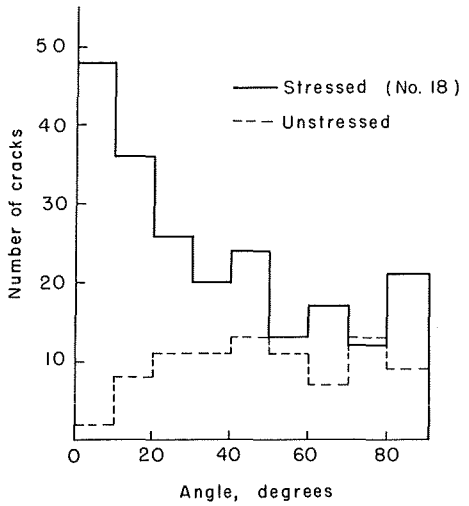

Fig. 11. Frequency distribution of crack orientation with respect to the direction of maximum compression in Westerly granite. The sample consisted of 80 cracks.

ently formed at the expense of those under 10 μm long, and that intermediate aspect ratios have become more significant, in stressed Westerly granite. The strong preferred orientation of LARCs evident in fields such as Fig. 3 is also shown by the histograms in Fig. 11. A definite peak is evident near the direction of maximum compression. Fields of the same size contained 217 LARCs in stressed material as opposed to 83 in unstressed; the latter showed no preferred orientation (Fig. 11).

Although the diabase was stressed nearly to fracture, most of the grain boundaries remained uncracked. In Fig. 9 a crack is shown which crossed an intact plagioclase–pyroxene boundary. Many intragranular cracks which emanate from the main crack are also visible. Other fields show that the mineral cleavage planes exert a strong influence in intragranular cracking.

Thermally stressed rock

Selected fields on the surface of a sample of Chelmsford granite were compared before and after heating to 400°C in air. One pair is shown in Figs. 10.

The bridges across the cracks were broken. Existing cracks extended and intersected, and some more than doubled in width. At some sharp corners which were present before heating, new cracks formed. The new cracks were observed at places which would be expected to be regions of high stress, for example grain boundaries, crack tips and corners. Many previously uncracked grain boundaries were opened. Within some of the large quartz grains there were many new intersecting cracks. Although the feldspars are relatively porous (about 2 per cent) the HARCs remained disconnected in the plane of observation.

DISCUSSION

Surface damage

Standard techniques of grinding and polishing nonmetallic solids may produce brittle cracks, local melting or plastic flow, and may leave an accumulation of debris. Ion thinning produces fewer of these effects than mechanical polishing, but it is important to know if any of the features we see under the SEM are due to thinning. Evidently the dimples noted earlier result from thinning, but do any of the cracks or other cavities? Several arguments suggest that damage due to thinning is negligible at the magnification we are using.

First, ion thinning is a technique currently used to produce the 0·1 μm thick foils for transmission electron microscopy ([21], for example). Here, images are magnified one or two orders of magnitude more than with the SEM, so that if thinning produced damage it would be even more obvious. In general, thinning introduces no cracks, gross lattice defects or glass; in a few cases round cavities about 50 Å in diameter are traceable to thinning [23]. Some heating occurs; it is of the order of 200° in the 0·1 μm foils. Presumably it would be much less in our case, for the surface of a solid specimen.

A second argument [3] is based on the preservation of delicate features such as the tiny bridges which span some of the cavities. Some of the material we now see in the larger cavities may well be debris from the original surface, although it would have had to percolate downward a distance equal to 50–100 times the opening of the cavity. Finally, in rocks which have negligible crack porosity based on elastic measurements (gabbro, or diabase, for example), crack-like cavities are rarely seen with the SEM. Presumably surface damage produces sharp-ended, brittle cracks; these are very uncommon in unstressed specimens prepared with the ion thinner. We conclude, therefore, that we are viewing an essentially undisturbed section, which reveals the microcavities as they occur in the interior of the specimen.

Techniques of crack mapping

We now assess various other techniques used to identify and map cracks in rocks. A major and somewhat unexpected finding in the present work was the small size, both length and width, of microcavities in rocks like granite. LARCs vary in length (Table 1); they rarely exceed a tenth the grain size, however. Width of cavities of all shapes uncommonly exceeds 1 μm. Features this small will almost certainly suffer from conventional surface preparation, which penetrates at least several μm [24]. Probably bridges will be destroyed and systems of cavities joined into single much longer features. Some material will be plucked, leaving holes, whereas grinding debris may fill existing cavities, obscuring them.

Of existing techniques, study of polished sections [9, 13] may be least affected by surface preparation. In contrast to a thin section, only a single surface is prepared; furthermore, the solid specimen offers some support to the surface material. However, even polished surfaces become damaged on a scale which may be critical for observation of microcavities. In addition, the small size of microcavities suggests that most will be well below the resolution of optical microscopes.

Preparation damage may be even more severe for thin sections owing to the mechanical stresses involved during handling of the thin rock slice. An indication of the damage from sectioning is given by reports of transgranular cracks [5, 7]. Apart from Red Lake granodiorite, transgranular cracks are very rare in any of our unstressed rocks. Stress, particularly nonhydrostatic, introduces abundant transgranular cracks.

Decoration of cavities present before sectioning might seem to offer a means of distinguishing those cavities from features due to preparation, but the small size of cavities makes this difficult. Dyes will simply not be visible and ultrafine grained film will be required for autoradiography. Decoration is also complicated by the debris left by sectioning [11] and by uncertainty as to complete penetration of the decorating agent prior to sectioning.

The above comments apply particularly to unstressed rocks. Stress tends to enlarge microcavities so that beyond some stress level they will become much more readily detectable and mappable. In other words, once stress has altered the original cavities to a greater extent

than does surface preparation, then use of thin or polished section seems appropriate. Thus, the angular distribution of LARCs we observe in highly stressed rock (Fig. 10) differs in no essential detail from that observed elsewhere in thin section [5–9]. However, features like aspect ratio, cavity length and density should probably not be reported from thin or polished section even for stressed rocks, until comparison is made of fields in optical and scanning electron microscopes.

Crack and pore porosity

The concept of cracks and pores evolved for rocks because it helped explain how many properties change under pressure. *Cracks*, for example, explained the rapid increase in modulus [1] or the decrease in certain types of attenuation [25], or the curious way the water saturation affected compressional and shear velocity [17]. To explain saturation effects both on velocity and electrical and fluid conductivity, the cracks would have to interconnect in a network. *Pores* were as important as cracks for they could explain high pressure conductivity [14] as well as the difference which usually remained when crack porosity was subtracted from total porosity; again, some large fraction of the pores would have to be part of a continuous network.

The SEM combined with ion thinning allows us for the first time to test these ideas. Rocks apparently do contain low aspect ratio crack-like cavities; by applying compressive stress we can infer through bridge collapse that they partially close and, therefore, act like the theoretical elastic crack. LARCs do not have the simple geometry of isolated elliptical cracks, however; nor is it yet clear that they are interconnected like a theoretical network. Rocks also contain, in HARCs, abundant features which can play the role of pores, although as noted above, many of the intragranular HARCs may not be interconnected. Grain boundaries might seem to be more ideal locations; there, pores could be rows of high aspect-ratio slots (Fig. 5) or simply the blunt ends of the LARCs which do not completely close under pressure. Thus, the general concept of cracks and pores seems correct, at least for the present sampling of rocks. However, several more serious discrepancies appear if we consider in detail theoretical estimates of crack and pore parameters.

Crack length has on the basis of Griffith theory been estimated to be approximately the grain size [26]. Based on our present work (Table 1), this is seen to be in serious error. LARCs are typically about a tenth the grain size. For some granites, closely-spaced LARCs would give an overall cavity length (as in the stressed sample, Fig. 1, and the combined lengths shown in Fig. 7) near the grain size, and perhaps it is this length which is appropriate for strength theory; rows of LARCs are not seen in diabase, gabbro or quartzite [3], however. Crack length proportional to grain size was predicted both by strength theory and by low pressure elastic effects [27]. For granites this may be correct, but it needs to be checked for the particular rocks involved.

Crack aspect ratio, α, has been predicted from the pressure to close cracks [28], from attenuation due to fluids in cracks [29], and from fluid permeability [30]. An α close to 10^{-3} is often estimated. The α we obtain for the granites often attains this value (Fig. 8); α for gabbro and diabase is much less certain owing to the small number of LARCs. α is hardly constant, however; for Westerly granite, for which 80 observations of α are available (Fig. 8), there appears to be an almost continuous spectrum up to α of 1. A few observations for the other rocks show a similar trend. A tendency toward a bimodal distribution of α may be detected for unstressed granite; it is probably too weak to be significant.

One should now be able to compare crack aspect-ratio from direct observation, with values obtained from measurement of modulus combined with theory [4]. One major difficulty is apparent, however; its solution may require a refinement of existing experimental techniques. We showed above that, in effect, LARC aspect-ratio changed under compressive stress; it may also change under hydrostatic pressure applied to the boundaries of a sample. Properties like modulus which display what might be termed 'crack effects' may therefore be somewhat dependent on pressure history, at least near those pressures capable of breaking LARC bridges and causing other local damage. We do not know the magnitude of those pressures, but they may well be in the range of pressure normally used to 'season' a strain gaged sample for static elastic measurements. Pressure is frequently cycled to seat a metal jacket and to improve stability and reproducibility of a strain gage measurement. Thus, the static elastic property eventually measured may not be appropriate for the LARCs originally seen in the rock before the pressure cycle. Many elastic effects may be sensitive to pressure history including the modulus at zero pressure, the pressure to close cracks [28], as well as the distribution of crack aspect ratios [31, 32]. Presumably high pressure effects, inasmuch as they reflect intrinsic behavior, should not show this pressure history. One exception could be electrical resistivity of saturated rock.

As noted in [3], *crack and pore porosity* as observed directly with the SEM were qualitatively in accord with total porosity measured by immersion, and crack porosity measured by volumetric compression [27]. As discussed above for Chelmsford granite, pore porosity was in fair quantitative agreement, whereas crack porosity disagreed by a factor of 2. For the latter, the influence of pressure history may also be critical; the crack porosity has been measured in the usual way with seasoned strain gages. To make this comparison more meaningful another method of strain measurement may be required.

Origin of microcavities

Much of the porosity described above does not seem to belong to well-known categories. In fact, the variety and abundance of microcavities, particularly in granites, was somewhat surprising; it presents an aspect of these rocks not evident in either outcrop, hand specimen or thin section. To what is this porosity due? We suggest that it may be due to several different and unrelated

causes. First, the distribution, shape and apparent isolation of many of the intragranular HARCs suggest that they might have been sites of a residual fluid phase which remained after crystallization of these rocks. Some could have been the sites of fluid inclusions [33]. This possibility could be tested by a study of minerals from igneous and metamorphic rocks with widely differing geologic history. Grain boundary HARCs may have originated as suggested above, or as in the case of quartzite [3] be the last trace of sedimentary porosity; or, they may have formed through the process suggested below for LARCs.

Cursory examination of our sections showed that long rows of bridged LARCs were most commonly associated with quartz grains. Apart from the bridges and blunt ends, these LARC systems might be considered fractures caused by internal stress due to changes of pressure or temperature or through mechanical loading, during their early history. The volume change associated with the α–β transition as well as somewhat unique thermoelastic properties suggest that internal stress will be high near the contact of quartz with most other minerals [34].

The bridges and blunt ends could be the result of a 'healing' process which has altered original longer brittle fractures. In Al_2O_3 crystals, brittle fractures altered to tubular voids with round ends when the crystals were held at 1600–1800°C for some time [35], apparently through vapor transport or surface diffusion. Some cylindrical voids ultimately separated into rows of spherical pores. Bridged LARCs (Fig. 6) and some HARCs (Fig. 5) could reflect this sort of alteration, presumably in the presence of water, at much lower temperature.

Some isolated LARCs within feldspar (Fig. 5), mica or pyroxene may represent cleavage cracks; they are sometimes bridged, with rounded ends. Still another aspect of the LARCs was illustrated in [3]. The complex system of sharp-ended, discontinuous, delicately bridged LARCs at the boundary of two feldspar grains suggested ductile fracture of this material, presumably in response to stress acting during a very early stage in the history of the rock.

Further applications

Several features of our new technique suggest that it may have wide application. Details of pore shape and interior, of crack location and aspect-ratio are visible. Cracks and other damage suggestive of brittle behavior stand out in contrast to the microcavities already present in rocks. Little ambiguity remains in old (pre-existing) as opposed to new (introduced by sectioning or rough handling) crack-like cavities.

Certain microcavities and their arrangement may prove to be diagnostic of crystallization conditions for igneous rocks; this could mirror recent application of the SEM to the study of the sedimentary history of sands based on minute surface details of grains [36]. Some joint systems may be traceable to early (healed) fracture systems, whereas others may be linked to features ascribable to late, near-surface stress systems. Under nonhydrostatic stress, dilatancy occurs in rocks; its onset has been determined roughly from stress–strain behavior. It may be possible to locate the onset and, indeed, to trace the early development of a fault more accurately, using the present method.

CONCLUSIONS

(1) Removal by ion thinning of about 30 μm of material from a polished surface exposes microcavities in typical crystalline rocks as they exist in the interior of a specimen. Damage due to thinning itself is negligible at SEM magnification.

(2) Study of the ion-thinned surface using the SEM reveals cavities having a wide variety of lengths and aspect ratios. A string of long thin cavities (LARCs) often follows grain boundaries. Individual LARCs are usually 1/10 the grain size and up to about 1 μm wide. The amount of grain boundary occupied by LARCs varied among different rocks from zero (diabase) up to 90 per cent (some granite).

(3) Blunt, often rounded ends typify LARCs for rocks with no laboratory stress history. This form, in addition to the frequent bridges interrupting the LARCs, suggests a late alteration or 'healing' of cracks introduced early in the history of the rocks.

(4) Compressive stress or high temperature cause damage which stands out in contrast to features seen in original samples. Sharp-ended brittle cracks form, LARCs widen and often break through bridges to join, and transgranular LARCs become abundant.

(5) More nearly equant cavities (HARCs) are widespread in sodic plagioclase, less common within quartz and potash feldspar, and in irregular distribution in grain boundaries. They range up to a few μm in size and may represent the sites of fluid inclusions, the last trace of sedimentary porosity, or possibly a nearly complete 'healing' of early fractures.

(6) The small scale of most microcavities in unstressed rock limits measurement of length, aspect ratio and density to ion thinned samples. Once material has been highly stressed, new cracks are more readily detectable and use of thin or polished section is appropriate.

(7) The concept of cracks and pores seems correct in a general way. LARCs almost never have elliptical form or sharp ends, however, and often nearly adjoin one another. Damage to bridges subjected to compression shows that LARCs may play the role of elastic cracks, nonetheless.

(8) LARC lengths are much less than predicted by fracture experiments; both theory and experiments will have to be re-examined.

(9) LARC aspect ratio ranged from 1 to about 10^{-3} in accord with general predictions from crack theory and measurements of elasticity and permeability. Aspect ratios of 10^{-2} to 10^{-3} become more significant after compression of a rock.

(10) Based on changes in form of LARCs due to compression, the rôle of pressure history may be greater than

generally realized for rock properties which display so-called crack effects.

Received 20 *September* 1973.

Acknowledgements—This research was supported by the National Science Foundation under Grant 36280. Preparation of the manuscript was supported by the U.S. Army Research Office under Contract DAHCO4-73-C-0017. Kate Hadley and J. B. Walsh offered a number of helpful suggestions. The use of ion thinning was first suggested to us by Christopher Goetze.

REFERENCES

1. Adams L. H. and Williamson E. D. The compressibility of minerals and rocks at high pressure. *J. Franklin Inst.* **195,** 475–529 (1923).
2. Brace W. F. Pore pressure in geophysics. Geophysical Monograph No. 16, *Flow and Fracture of Rocks,* 265–274, John Wiley & Sons, New York (1972).
3. Brace W. F., Silver E., Hadley K. and Goetze C. Cracks and pores: A closer look. *Science Wash.* **178,** 162–164 (1972).
4. Walsh J. B. and Brace W. F. Cracks and pores in rocks. *Int. Congr. of Rock Mechanics, Lisbon,* 643–646 (1966).
5. Paulding B. W. Jr. Crack growth during brittle fracture in compression. PhD Thesis, Mass. Institute of Technology (1965).
6. Koide H. and Hoshino K. Development of microfractures in experimentally deformed rocks (Preliminary Report). *Jishin* **20,** 85–97 (1967).
7. Peng S. and Johnson A. M. Crack growth and faulting in cylindrical specimens of Chelmsford granite. *Int. J. Rock Mech. Min. Sci.* **9,** 37–86 (1972).
8. Willard R. J. and McWilliams J. R. Microstructural techniques in the study of physical properties of rocks. *Int. J. Rock Mech. Min. Sci.* **6,** 1–2 (1969).
9. Wawersik W. R. and Brace W. F. Post-failure behavior of granite and diabase. *Rock Mech.* **3,** 61–85 (1971).
10. Baldridge S. and Simmons G. Progress in microcrack decoration. *EOS Trans. Am. Geophys. Un.* **52** 342 (1971).
11. Fryer G. M. and Roberts J. P. Some techniques for microscopical examination of ceramic materials. *Trans. Br. Ceram. Soc.* **62,** 537–548 (1963).
12. Hadley K. Personal communication (1971).
13. Timur A., Hempkins W. B. and Weinbrandt R. M. Scanning electron microscope study of pore systems in rocks. *J. Geophys. Res.* **76,** 4932–4948 (1971).
14. Brace W. F., Orange A. S. and Madden T. R. The effect of pressure on the electrical resistivity of water-saturated crystalline rocks. *J. Geophys. Res.* **70**(22), 5669–5678 (1965).
15. Birch F. The velocity of compressional waves in rocks to 10 kb, I. *J. Geophys. Res.* **65,** 1083 (1960).
16. Brace W. F. and Orange A. S. Further studies of the effects of pressure on electrical resistivity of rocks. *J. Geophys. Res.* **73,** 5407–5420 (1968).
17. Nur A. and Simmons G. The effect of saturation on velocity in low porosity rocks. *Earth Planet. Sci. Lett.* **7,** 183–193 (1969).
18. Kimoto S. and Russ J. C. The characteristics and applications of the scanning electron microscope, *Amer. Scient.* **57,** 112 (1969).
19. Majumdar A. J. The application of scanning electron microscopy to textural studies. *Proc. Br. Ceram. Soc.* **20,** 43–69 (1970).
20. Oatley C. W., Nixon W. C. and Pease R. F. W. Scanning electron microscopy, in *Advances in Electronics and Electron Physics,* **21,** 181–247, Academic Press, New York (1965).
21. Sprunt E. Scanning electron microscope study of cracks and pores in crystalline rocks. MS Thesis, Mass. Institute of Technology (1973).
22. Heuer A. H., Firestone R. F., Snow J. D., Green H. W., Howe R. G. and Christie J. M. An improved ion-thinning apparatus. *Rev. Sci. Inst.* **42,** 1177–1184 (1971).
23. Vander Sande J. Personal communication (1973).
24. Bowden F. P. and Tabor D. *The Friction and Lubrication of Solids,* Part II, 15, Oxford University Press (1964).
25. Walsh J. B. Seismic wave attenuation in rock due to friction. *J. Geophys. Res.* **71,** 2591–2599 (1966).
26. Brace W. F. Brittle fracture of rocks, in *State of Stress in the Earth's Crust,* Ed. W. R. Judd, 110–178, Elsevier, New York (1964).
27. Brace W. F. Some new measurements of linear compressibility of rocks. *J. Geophys. Res.* **70,** 391–398 (1965).
28. Walsh J. B. Behavior of rock salt, limestone and anhydrite during indentation. *J. Geophys. Res.* **65,** 1773–1788 (1960).
29. Nur A. and Simmons G. The effect of viscosity of a fluid phase on velocity in low porosity rocks. *Earth Planet. Sci. Lett.* **7,** 99–108 (1969).
30. Brace W. F., Walsh J. B. and Frangos W. T. Permeability of granite under high pressure. *J. Geophys. Res.* **73,** 2225–2236 (1968).
31. Walsh J. B. and Decker E. R. Effect of pressure and saturating fluid on the thermal conductivity of compact rock. *J. Geophys. Res.* **71,** 3052–3061 (1966).
32. Morlier P. Description de l'état de fissuration d'une roche à partir d'essais non-destructifs simples. *Rock Mech.* **3,** 125–138 (1971).
33. Roedder E. Composition of fluid inclusions. U.S. Geol. Survey Prof. Paper 440-JJ, 250 pp. (1972).
34. Nur A. and Simmons G. The origin of small cracks in igneous rocks. *Int. J. Rock Mech. Min. Sci.* **7,** 307–314 (1970).
35. Yen C. F. and Coble R. L. Spheroidization of tubular voids in Al_2O_3 crystals at high temperatures. *J. Am. Ceram. Soc.* **55,** 507–509 (1972).
36. Krinsley D. H. and Margolis S. V. A study of quartz sand grain surface textures with the scanning electron microscope. *Trans. N.Y. Acad. Sci.* **31,** 457–460 (1969).